

# Melting relations of multicomponent carbonate $\text{MgCO}_3\text{--FeCO}_3\text{--CaCO}_3\text{--Na}_2\text{CO}_3$ system at 12–26 GPa: application to deeper mantle diamond formation

Anna Spivak<sup>1</sup> · Natalia Solopova<sup>3</sup> · Leonid Dubrovinsky<sup>2</sup> · Yuriy Litvin<sup>3</sup>

Received: 4 March 2015 / Accepted: 1 July 2015 / Published online: 26 July 2015  
© Springer-Verlag Berlin Heidelberg 2015

**Abstract** Carbonatic components of parental melts of the deeper mantle diamonds are inferred from their primary inclusions of (Mg, Fe, Ca, Na)-carbonate minerals trapped at *PT* conditions of the Earth's transition zone and lower mantle. *PT* phase diagrams of  $\text{MgCO}_3\text{--FeCO}_3\text{--CaCO}_3\text{--Na}_2\text{CO}_3$  system and its ternary  $\text{MgCO}_3\text{--FeCO}_3\text{--Na}_2\text{CO}_3$  boundary join were studied at pressures between 12 and 24 GPa and high temperatures. Experimental data point to eutectic solidus phase relations and indicate liquidus boundaries for completely miscible (Mg, Fe, Ca, Na)- and (Mg, Fe, Ca)-carbonate melts. *PT* fields for partial carbonate melts associated with (Mg, Fe)-, (Ca, Fe, Na)-, and ( $\text{Na}_2\text{Ca}$ ,  $\text{Na}_2\text{Fe}$ )-carbonate solid solution phases are determined. Effective nucleation and mass crystallization of deeper mantle diamonds are realized in multicomponent (Mg, Fe, Ca, Na)-carbonatite–carbon melts at 18 and 26 GPa. The multicomponent carbonate systems were melted at temperatures that are lower than the geothermal ones. This gives an evidence for generation of diamond-parental carbonatite melts and formation of diamonds at the *PT* conditions of transition zone and lower mantle.

**Keywords** Mg–Fe–Ca–Na-carbonate system · Melting *PT* phase diagram · Deeper mantle diamond formation · Experiment

## Introduction

Deeper mantle diamonds of the transition zone and lower-mantle origin are rare but important “strangers” at the Earth's surface carrying crucial information about deep interiors. The diamonds contain primary inclusions of Mg–Fe–Al- and Ca–Fe-silicates as well as Mg–Fe- and Si-oxides which are expected in the Earth's lower mantle due to experimental estimates (Akaogi 2007; Harte 2010). Moreover, the diamonds have primary mineral inclusions of different (Mg, Fe, Ca, Na)-carbonates (McCammon et al. 1997; Brenker et al. 2007; Kaminsky 2012). This indicates that carbonate components are presented in the diamond-parental media of the Earth's transition zone and lower mantle and can be inferred from primary inclusions.

Previous experimental works showed that solid carbonates of magnesium, calcium, iron, and sodium are stable at a wide interval of *PT* conditions along the mantle geotherm (Fiquet et al. 2002; Santillan and Williams 2004a, b; Isshiki et al. 2004; Skorodumova et al. 2005; Dasgupta and Hirschmann 2010; Stagno et al. 2011; Merlini et al. 2012). It is assumed that carbonates could be a significant compounds at the conditions of the Earth's deep interiors (Fiquet et al. 2002; Isshiki et al. 2004; Dasgupta and Hirschmann 2010; Stagno et al. 2011; Boulard et al. 2011).

Mineralogical data on primary inclusions in deeper mantle diamonds provide information about a general chemical composition of diamond-parental medium but could not reveal the substance responsible for diamonds origin. The

✉ Anna Spivak  
spivak@iem.ac.ru

<sup>1</sup> Present Address: Institute of Experimental Mineralogy, Russian Academy of Sciences, Academician Oshp'yan Str. 4, Chernogolovka, Moscow Region, Russia

<sup>2</sup> Bayerisches Geoinstitut, University of Bayreuth, Bayreuth, Germany

<sup>3</sup> Institute of Experimental Mineralogy, Russian Academy of Sciences, Academician Oshp'yan Str. 4, Chernogolovka, Moscow Region, Russia

**Table 1** Conditions and results of experiments with multicomponent carbonate  $\text{FeCO}_3\text{--MgCO}_3\text{--Na}_2\text{CO}_3$  system

Experimental run	P, GPa <sup>a</sup>	T, °C <sup>a</sup>	Duration of heating, min	Products of the experiments			
				Phase	Sid (mol%)	Mgs (mol%)	Nc (mol%)
H3774	12	1000	30	(Nc·Sid·Mgs) <sub>s.s.</sub>	0.24	0.13	0.63
				(Nc·Sid·Mgs) <sub>s.s.</sub>	0.09	0.34	0.57
				(Sid·Mgs) <sub>s.s.</sub>	0.46	0.53	0.01
				(Sid·Mgs) <sub>s.s.</sub>	0.60	0.39	0.01
H3781	12	1150	30	L	0.26	0.11	0.63
				(Nc·Sid·Mgs) <sub>s.s.</sub>	0.13	0.30	0.57
				(Sid·Mgs) <sub>s.s.</sub>	0.39	0.58	0.03
				(Sid·Mgs) <sub>s.s.</sub>	0.47	0.49	0.04
H3770	12	1300	20	L	0.17	0.19	0.64
H3796	18	800	60	(Nc·Sid·Mgs) <sub>s.s.</sub>	0.12	0.41	0.48
				(Nc·Sid·Mgs) <sub>s.s.</sub>	0.19	0.03	0.77
				(Nc·Sid·Mgs) <sub>s.s.</sub>	0.39	0.07	0.54
				(Sid·Mgs) <sub>s.s.</sub>	0.37	0.59	0.04
				(Sid·Mgs) <sub>s.s.</sub>	0.57	0.35	0.08
H3794	18	1000	30	(Nc·Sid·Mgs) <sub>s.s.</sub>	0.32	0.12	0.56
				(Sid·Mgs) <sub>s.s.</sub>	0.26	0.71	0.03
				(Sid·Mgs) <sub>s.s.</sub>	0.54	0.44	0.02
S5816	18	1300	30	L	0.35	0.11	0.54
				(Sid·Mgs) <sub>s.s.</sub>	0.44	0.53	0.02
S5905	18	1650	20	L	0.26	0.26	0.48
				(Sid·Mgs) <sub>s.s.</sub>	0.70	0.29	0.01
H3937	18	1800	10	L	0.36	0.24	0.40

<sup>a</sup> Uncertainty in pressure and temperature is  $\pm 0.5$  GPa and  $\pm 50$  °C, respectively. Phase composition of the experimental products expressed in mole %. Sid— $\text{FeCO}_3$ , Mgs— $\text{MgCO}_3$ , Nc— $\text{Na}_2\text{CO}_3$

chemical composition of parental medium and mechanism of diamonds formation may be understood based on results of physicochemical experiments and a syngensis criterion of diamonds and inclusions (Litvin 2007). The criterion demands parental medium to provide conditions for joint formation of diamonds and complete set of paragenetic inclusions as well as make the possibility for the presence of xenogenetic phases.

The main objectives of this work are experimental studies: (1) melting phase relations of multicomponent carbonate  $\text{MgCO}_3\text{--FeCO}_3\text{--CaCO}_3\text{--Na}_2\text{CO}_3$  system and its ternary  $\text{MgCO}_3\text{--FeCO}_3\text{--Na}_2\text{CO}_3$  boundary join (with representative carbonate components of primary inclusions in deeper mantle diamond), in particular to determine the solidus and liquidus boundaries, (2) a diamond-forming efficiency of the multicomponent carbonate melts, mechanisms of formation of diamonds and paragenetic carbonate minerals in carbonate–carbon melt solutions under conditions of partial and complete melting, and correspondence of results to the syngensis criterion.

## Methods

Experimental study on melting of multicomponent carbonate systems was carried out using high-pressure, high-temperature 1200 t (Sumitomo) multianvil hydraulic press at pressures between 12 and 26 GPa and temperatures from 800 to 1800 °C at BGI (Bayerisches Geoinstitute, Bayreuth, Germany). The conditions and result of the experiments are summarized in Tables 1 and 2. Standard 14/8, 10/5, 10/4, and 7/3 cell assemblages for pressures of 12, 18, 23, and 26 GPa, respectively, were used. The experimental assemblages and procedures have been earlier described by Frost et al. (2004). We used synthetic magnesite  $\text{MgCO}_3$  (99.9 % purity), calcite  $\text{CaCO}_3$  (99.9 %),  $\text{Na}_2\text{CO}_3$  (99.9 %), and natural siderite with composition  $(\text{Fe}_{0.98}\text{Mn}_{0.02})\text{CO}_3$  as starting materials. All starting carbonates have been dried for at least 24 h at temperature 250 °C. A starting mixture was placed into a capsule made of a rhenium foil. High temperature was generated using a  $\text{LaCrO}_3$  heater. Immediate quenching was applied after heating regime. Accuracies

**Table 2** Conditions and results of experiments with multicomponent carbonate  $\text{FeCO}_3\text{--MgCO}_3\text{--CaCO}_3\text{--Na}_2\text{CO}_3$  system

Experimental run	P, GPa <sup>a</sup>	T, °C <sup>a</sup>	Duration of heating, min	Products of the experiments				
				Phase	Sid (mol%)	Mgs (mol%)	Cal (mol%)	Nc (mol%)
S5857	12	800	120	(Nc·Cal·Sid) <sub>s,s</sub>	0.11	0.04	0.30	0.55
				(Cal·Sid·Nc) <sub>s,s</sub>	0.10	0.03	0.67	0.21
				(Sid·Mgs) <sub>s,s</sub>	0.58	0.40	0.01	0.01
				(Sid·Mgs) <sub>s,s</sub>	0.71	0.27	0.02	0.01
S5906	12	1000	120	L	0.09	0.05	0.40	0.43
				(Nc·Cal·Sid) <sub>s,s</sub>	0.11	0.06	0.21	0.62
				(Cal·Nc·Sid) <sub>s,s</sub>	0.10	0.05	0.62	0.23
				(Sid·Mgs) <sub>s,s</sub>	0.31	0.66	0.03	0.01
S5860	12	1150	30	L	0.10	0.06	0.38	0.46
				(Cal·Nc·Sid) <sub>s,s</sub>	0.15	0.08	0.37	0.39
				(Sid·Mgs) <sub>s,s</sub>	0.34	0.61	0.04	0.01
S5872	12	1300	10	L	0.12	0.06	0.31	0.50
				(Sid·Mgs) <sub>s,s</sub>	0.33	0.62	0.04	0.01
S5870	12	1400	10	L	0.15	0.09	0.41	0.35
				(Sid·Mgs) <sub>s,s</sub>	0.28	0.67	0.04	0.01
S5871	12	1650	5	L	0.19	0.26	0.27	0.29
S5885	23	1050	30	(Nc·Cal·Sid) <sub>s,s</sub>	0.10	0.02	0.53	0.36
				(Cal·Nc·Sid) <sub>s,s</sub>	0.10	0.04	0.66	0.20
				(Sid·Mgs) <sub>s,s</sub>	0.54	0.45	0.01	0.01
S5893	23	1250	20	L	0.11	0.06	0.43	0.40
				(Nc·Cal·Sid) <sub>s,s</sub>	0.12	0.07	0.20	0.60
				(Cal·Nc·Sid) <sub>s,s</sub>	0.12	0.05	0.61	0.22
				(Sid·Mgs) <sub>s,s</sub>	0.47	0.50	0.02	0.02
S5892	23	1450	20	L	0.10	0.05	0.33	0.51
				(Sid·Mgs·Cal·Nc) <sub>s,s</sub>	0.24	0.39	0.20	0.17
				(Sid·Mgs) <sub>s,s</sub>	0.30	0.66	0.03	0.01
S5877	23	1650	10	L	0.16	0.07	0.21	0.56
				(Sid·Mgs) <sub>s,s</sub>	0.33	0.63	0.04	0.01
S6024	23	1800	5	L				

<sup>a</sup> Uncertainty in pressure and temperature is  $\pm 0.5$  GPa and  $\pm 50$  °C, respectively. Phase composition of the experimental products expressed in mole %. Sid— $\text{FeCO}_3$ , Mgs— $\text{MgCO}_3$ , Cal— $\text{CaCO}_3$ , Nc— $\text{Na}_2\text{CO}_3$

of pressure and temperature determination were estimated as  $\pm 0.5$  GPa and  $\pm 50$  °C, respectively.

Chemical compositions of starting carbonate systems used for melting phases relation studies were prepared by mixing of: (1)  $\text{FeCO}_3\text{—}35$ ;  $\text{MgCO}_3\text{—}35$ ;  $\text{Na}_2\text{CO}_3\text{—}30$  wt% and (2)  $\text{FeCO}_3\text{—}26$ ;  $\text{MgCO}_3\text{—}26$ ;  $\text{CaCO}_3\text{—}25$ ;  $\text{Na}_2\text{CO}_3\text{—}23$  wt%. The model compositions take into account mineralogical data of representative carbonate minerals within the primary inclusions in diamonds, especially, from the upper part of the lower mantle (Kaminsky 2012).

Mixtures of the compositions ( $\text{Mg}$ ,  $\text{Fe}$ ,  $\text{Na}$ -carbonates)<sub>60</sub>carbon<sub>40</sub> and ( $\text{Mg}$ ,  $\text{Fe}$ ,  $\text{Ca}$ ,  $\text{Na}$ -carbonates)<sub>60</sub>carbon<sub>40</sub> were used for study of diamond crystallization. Elemental carbon is graphite that is a metastable phase in experimental conditions of diamond crystallization in carbonate–carbon systems at 18 GPa and 1800 °C (transition zone conditions) as well as 26 GPa

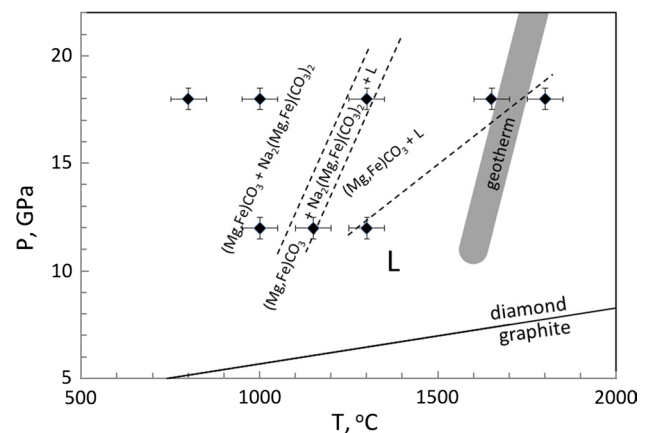


**Fig. 1** *PT* phase diagram of  $\text{MgCO}_3\text{--FeCO}_3\text{--Na}_2\text{CO}_3$  system. *Black diamonds* experimental points, *dashed lines* curves of phase fields, *black line* equilibrium boundary diamond/graphite (Bundy et al. 1996), *thick gray line* geotherm (Stacey 1992)

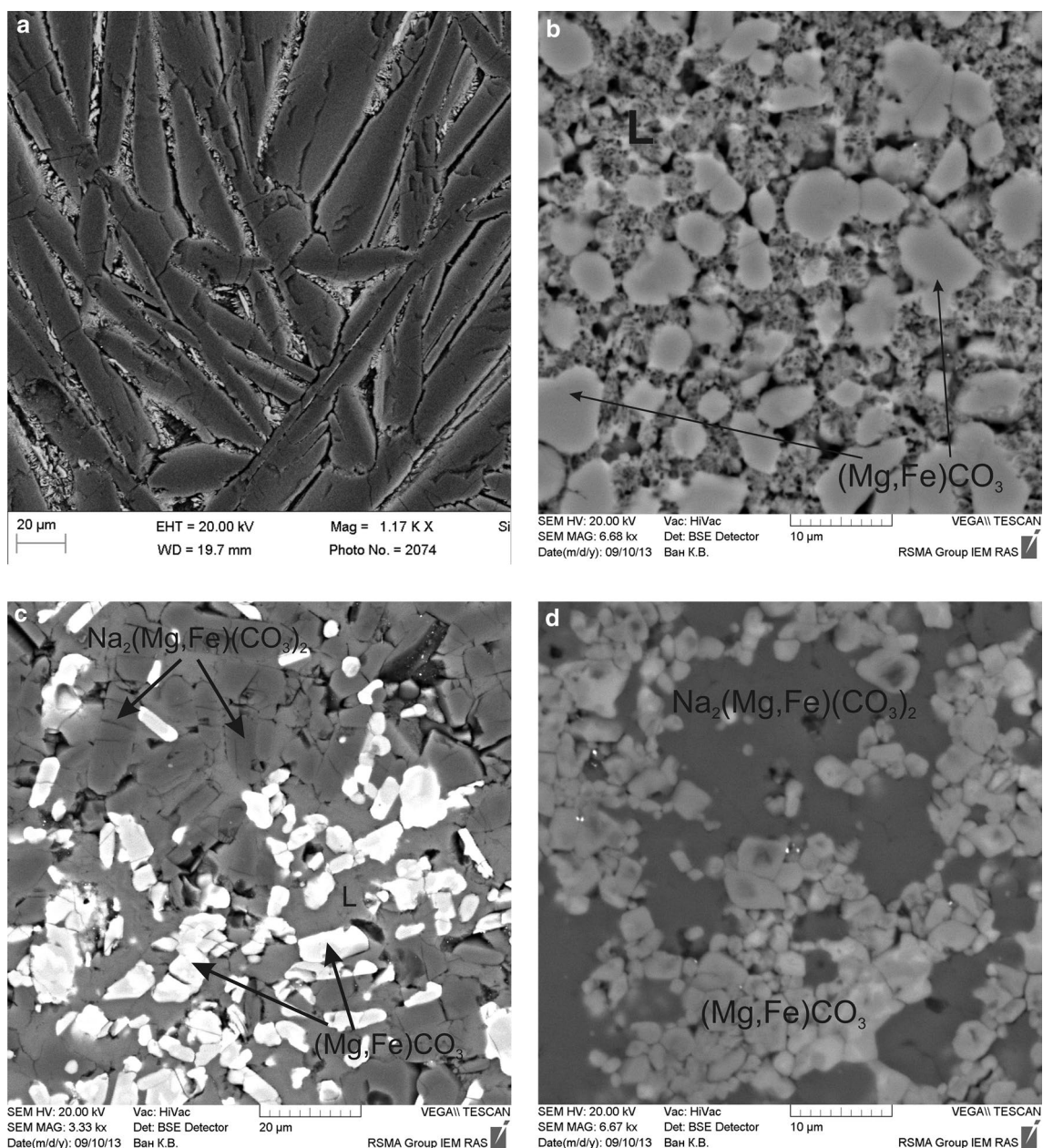


**Fig. 2** SEM images of experimental samples of melting relations of multicomponent carbonate system  $\text{FeCO}_3\text{--MgCO}_3\text{--CaCO}_3\text{--Na}_2\text{CO}_3$ : **a** 1300 °C, 12 GPa (# H3770); **b** 1650 °C, 18 GPa (# S5905); **c** 1150 °C, 12 GPa (# H3781); **d** 1000 °C, 18 GPa (# H3794)

and 1900 °C (lower-mantle conditions). Metastability of graphite under these conditions is demonstrated by experimental carbon phase diagram for both stable and metastable solid carbon phases (Bundy et al. 1996). The diagram and corresponding experimental data demonstrate that the metastable graphite is not capable to transform into diamond by mechanism of direct transition in spite of the conditions belong to the diamond thermodynamic stability field. Under experimental *PT* conditions used in this work, carbonate liquids play a key role in diamond formation because they are capable to dissolve elemental

carbon. The parental carbonate + graphite (and/or diamond formed) mixes and resulted melts form strong buffer couples with  $f_{\text{O}_2}$  close to the  $\text{FeO}/\text{Fe}$  buffer (Litvin et al. 2008).

Compositions of experimental phases and textural relationships were characterized using a scanning electron microscope Tescan Vega II XMU equipped EDS (INCAx-sight), at an accelerating voltage of 20 kV, beam current up to 450 pA, the size of the electron beam 210 nm at the Institute of Experimental Mineralogy of the RAS in Chernogolovka, Moscow region.

## Results and discussion

Melting relations in the systems  $\text{MgCO}_3\text{--FeCO}_3\text{--Na}_2\text{CO}_3$  and  $\text{MgCO}_3\text{--FeCO}_3\text{--CaCO}_3\text{--Na}_2\text{CO}_3$  were experimentally studied at 12–23 GPa and 800–1800 °C. Experimental conditions and results are presented in Tables 1 and 2 for the multicomponent carbonate  $\text{FeCO}_3\text{--MgCO}_3\text{--Na}_2\text{CO}_3$  and  $\text{MgCO}_3\text{--FeCO}_3\text{--CaCO}_3\text{--Na}_2\text{CO}_3$  systems, respectively.

Melting relations of the system  $\text{MgCO}_3\text{--FeCO}_3\text{--Na}_2\text{CO}_3$  are shown in Fig. 1. The  $PT$  phase fields are limited by a lower temperature boundary (1100 °C at 12 GPa) of eutectic melting of the multiphase carbonate system and a higher boundary of complete melting at temperature 1700 °C at 18 GPa. The experimental data are extrapolated within 11–24 GPa. Single-phase field of completely miscible Mg–Fe–Na-carbonate melt is restricted by the liquidus line. The quenched melts (Fig. 2b–c) are composed of relatively high contents of Na (0.64–0.40 mol%  $\text{Na}_2\text{CO}_3$ ), Fe (0.36–0.17 mol%  $\text{FeCO}_3$ ), and Mg (0.24–0.19 mol%  $\text{MgCO}_3$ ) components. Liquidus phase is presented by solid solution phase of (Mg, Fe)-carbonate (Mg, Fe) $\text{CO}_3$  (Fig. 2b) with composition 0.47–0.39 mol%  $\text{FeCO}_3$  and 0.58–0.24 mol%  $\text{MgCO}_3$  and admixed 0.01–0.04 mol%  $\text{Na}_2\text{CO}_3$ . The quenched melts are characterized by  $\text{FeCO}_3$  (0.35–0.26 mol%),  $\text{MgCO}_3$  (0.26–0.11 mol%), and increasing  $\text{Na}_2\text{CO}_3$  (0.63–0.54 mol%) contents. At lower temperatures, a solid solution of Na–Mg–Fe-carbonate is formed composed (mol%) of  $\text{Na}_2\text{CO}_3$  (0.56–0.77),  $\text{FeCO}_3$  (0.09–0.32), and  $\text{MgCO}_3$  (0.41–0.03). Herewith, an invariant eutectic assemblage of (Mg, Fe)-carbonate + Na–Mg–Fe-carbonate + melt (L) is resulted (Fig. 2c). A subsolidus assemblage consists of (Mg, Fe)- and ( $\text{Na}_2\text{Mg}$ ,  $\text{Na}_2\text{Fe}$ )-carbonate phases (Fig. 2d).

Melting relations of the multicomponent carbonate system  $\text{MgCO}_3\text{--FeCO}_3\text{--CaCO}_3\text{--Na}_2\text{CO}_3$  are demonstrated in Fig. 3. A partial melting field is located between the boundaries of low-temperature eutectics (900 °C at 12 GPa) and complete melting (1700 °C at 23 GPa) at higher temperature. One-phase field of completely miscible multicomponent carbonate melt is next to the liquidus line (Fig. 4a). In partial melting fields, the compositions (mol%) of quenched melts are variable as 0.26–0.19  $\text{FeCO}_3$ , 0.26–0.24  $\text{MgCO}_3$ , 0.27  $\text{CaCO}_3$ , and 0.29–0.24  $\text{Na}_2\text{CO}_3$ . Mg–Fe-carbonate solid solutions is the liquidus phase of compositions (mol%) 0.33–0.28  $\text{FeCO}_3$  and 0.67–0.63  $\text{MgCO}_3$  with admixed  $\text{CaCO}_3$  up to 0.4 mol% and  $\text{Na}_2\text{CO}_3$  up to 0.1 mol% (Fig. 4b). At lower temperatures, the assemblage (Mg, Fe)-carbonate + Ca–Na–Fe–Mg-carbonate + melt appears (Fig. 4c). In this case, Ca–Na–Fe–Mg-carbonates are characterized by contents (mol%) of  $\text{CaCO}_3$  (0.66–0.61),  $\text{Na}_2\text{CO}_3$  (0.22–0.20), and  $\text{FeCO}_3$  (0.12–0.10) and admixed  $\text{MgCO}_3$  (less than 0.5). An invariant eutectic assemblage (Mg, Fe)-carbonate + (Ca,

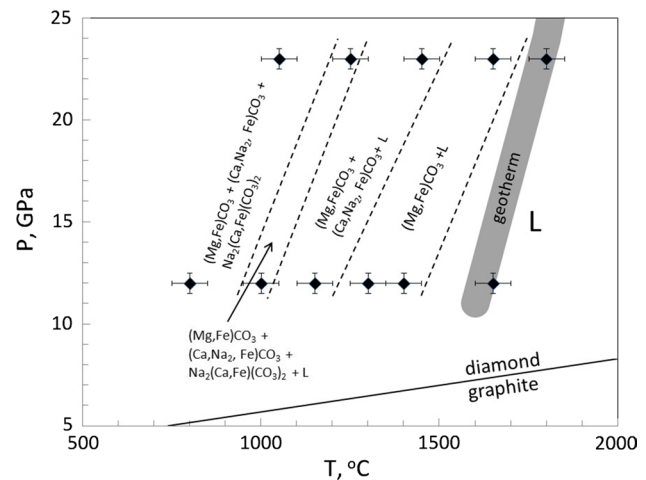


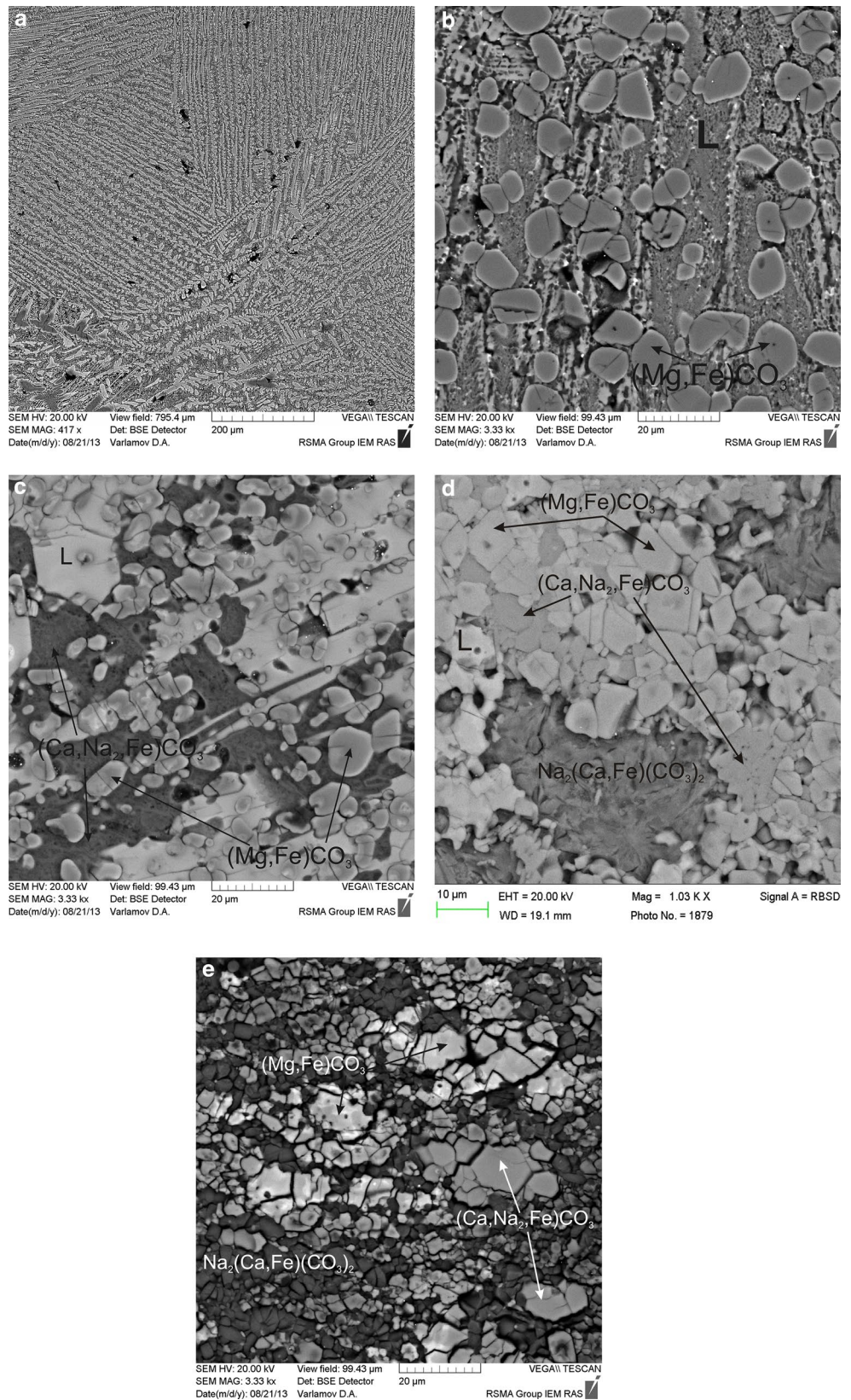
**Fig. 3**  $PT$  phase diagram of  $\text{MgCO}_3\text{--FeCO}_3\text{--CaCO}_3\text{--Na}_2\text{CO}_3$  system. Black diamonds experimental points, dashed lines curves of phase fields, black line equilibrium boundary diamond/graphite (Bundy et al. 1996), thick gray line geotherm (Stacey 1992)

Na, Fe, Mg)-carbonate + ( $\text{Na}_2\text{Ca}$ ,  $\text{Na}_2\text{Fe}$ ,  $\text{Na}_2\text{Mg}$ )-carbonate + melt (Fig. 4d) which is determining for subsolidus assemblage (Mg, Fe) $\text{CO}_3$  + (Ca,  $\text{Na}_2$ , Fe, Mg)  $\text{CO}_3$  +  $\text{Na}_2$  (Ca, Fe, Mg)( $\text{CO}_3$ ) $_2$  is formed (Fig. 4e). Compositions (mol%) of  $\text{Na}_2$  (Ca, Fe, Mg)( $\text{CO}_3$ ) $_2$ -carbonates are variable within 0.62–0.60 for  $\text{Na}_2\text{CO}_3$ , 0.21–0.20 for  $\text{CaCO}_3$ , 0.12–0.11 for  $\text{FeCO}_3$  with about 0.07 for  $\text{MgCO}_3$ .

Crystallization of the deeper mantle diamonds in partially and completely melted carbonate systems  $\text{MgCO}_3\text{--FeCO}_3\text{--Na}_2\text{CO}_3\text{--C}$  and  $\text{MgCO}_3\text{--FeCO}_3\text{--CaCO}_3\text{--Na}_2\text{CO}_3\text{--C}$  (with dissolved elementary carbon) was experimentally realized at 18–26 GPa and 1800–1900 °C (Fig. 5). The dissolution of metastable graphite leads to the formation of carbon oversaturated in respect to diamond carbonate–carbon melt solution. The carbon-oversaturated state of carbonate–carbon melt is responsible for nucleation and mass crystallization of diamond (Litvin 2007). Experimental samples were liked as light gray solid aggregates consisting of diamond crystals (up to 34–40 vol %) in quenching carbonatic array. It should be noted that metastable graphite was sometime formed by similar mechanism as laminar single crystals together with diamonds (by SEM and Raman-spectroscopy data). Diamond crystals usually are bright, translucent octahedral individuals with flat faces and have a size of up to 30  $\mu\text{m}$ . Size of diamond crystals is reduced to first microns with increasing pressure. Clusters of diamond crystals up to 10 individuals were observed. In some cases, spinel twins and splices were found.

Growth of diamonds occurs in sectors of the octahedron faces (like natural diamonds). The rate of spontaneous crystallization of diamond is essential and sensitive to changes in pressure and temperature. The maximum rate of diamond

**Fig. 4** SEM images of experimental samples of multicomponent carbonate system  $\text{FeCO}_3$ – $\text{MgCO}_3$ – $\text{CaCO}_3$ – $\text{Na}_2\text{CO}_3$ : **a** 1650 °C, 12 GPa (# S5871); **b** 1650 °C, 23 GPa (# S5877); **c** 1150 °C, 12 GPa (# S5860); **d** 1250 °C, 23 GPa (# S5893); **e** 800 °C, 12 GPa (# S5857)



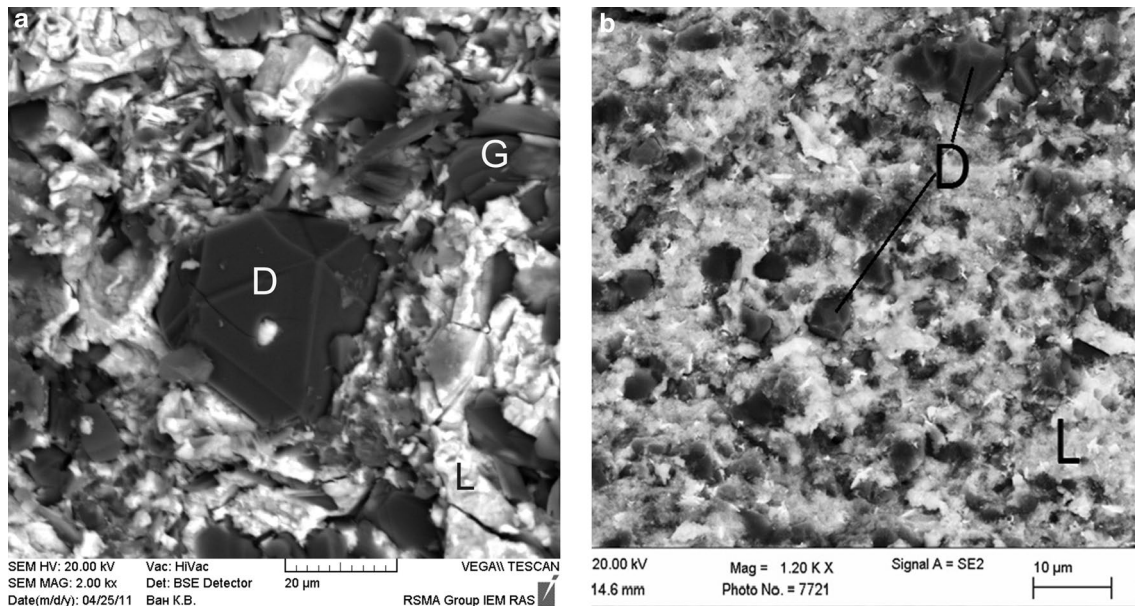


**Fig. 5** SEM images of experimental samples with synthesised of diamond in **a**  $\text{MgCO}_3\text{-FeCO}_3\text{-Na}_2\text{CO}_3\text{-C}$  system at 18 GPa and 1800 °C; **b**  $\text{MgCO}_3\text{-CaCO}_3\text{-FeCO}_3\text{-Na}_2\text{CO}_3\text{-C}$  system at 26 GPa

and 1900 °C. Crystals of diamond (D) and graphite (G) in quenched carbonate melt (L) are clearly visible

spontaneous crystallization is observed at very high pressures. The rate is decreased with a pressure decreasing; it is accompanied by a decrease in both the nucleation density and growth rates of single crystals, increasing their size.

Carbonate–carbon parental melts provide a simultaneous formation of deeper mantle diamonds and paragenetic carbonate minerals. Diamond nucleation and crystal growth are conditioned by generation of completely miscible carbonate melts oversaturated with dissolved carbon in respect of diamond. Hence, the oversaturated carbon is source for diamond, whereas the paragenetic carbonate minerals are crystallized from the melted carbonate solvents.

Carbonatitic (carbonate–silicate) composition of the upper-mantle parental media for majority of diamonds and their primary inclusions was proven based on experimental studies and field observations (Litvin 2007, 2009; Litvin et al. 2012). Based on the syngensis criterium of diamond and inclusions, parental (growth) media of deeper mantle diamonds are postulated as carbonate–oxide–silicate–carbon systems in partially molten state at conditions of the lower mantle (Litvin et al. 2014). This is compatible with the mantle-carbonatite version of the upper-mantle diamond genesis.

Study of melting phase relations of the multicomponent carbonates trapped into deeper mantle diamonds is of fundamental importance for characterization of their genesis. Congruent melting of simple carbonates  $\text{CaCO}_3$ ,  $\text{MgCO}_3$ , and  $\text{Na}_2\text{CO}_3$  and stability of their melts over a wide *PT* range of the transition zone and lower mantle was earlier

revealed by experimental investigations (Spivak et al. 2011, 2012, 2013; Solopova et al. 2013; Litvin et al. 2014). It was also found that molten carbonate–carbon systems are very effective as diamond-forming media. At the same time, the carbonate melts are effective solvents and growth media for oxide and silicate minerals of the transition zone and lower mantle. Multicomponent carbonate melts studied in this work are composed of components of all the carbonate minerals included into deeper mantle diamonds and thus may be considered as representatives of carbonatitic constituents of parental media for the transition zone and lower-mantle diamonds. This is supported by preliminary experiments on diamond crystallization in multicomponent oxide–silicate–carbonate–carbon melts within lower-mantle pressures of 23–26 GPa (Litvin et al. 2014).

## Concluding remarks

High-pressure high-temperature experiments on the  $\text{MgCO}_3\text{-FeCO}_3\text{-Na}_2\text{CO}_3$  and  $\text{MgCO}_3\text{-FeCO}_3\text{-CaCO}_3\text{-Na}_2\text{CO}_3$  systems demonstrate (Figs. 1, 3) that multicomponent carbonate melts are completely miscible and stable under the transition zone and lower-mantle conditions. The *PT* parameters of the partial melting of the system are compatible with the transition zone conditions: The melts starts to form at temperatures noticeably lower than the geothermal ones. The positive superposition of geothermal and primary melting conditions is determining in the formation

of the transition zone and lower-mantle diamond-parental melts, nucleation, and mass crystallization of deeper mantle diamonds in the parental carbonate–silicate–oxide–carbon melts (Litvin et al. 2014).

The multicomponent Mg–Fe–Na- and Mg–Fe–Ca–Na-carbonatitic melts provide perfect environment for deeper mantle diamond formation. As shown in Figs. 1 and 3, carbonates and diamonds may form paragenetic associations at conditions of partial carbonates melting. Thus, it was revealed that temperatures of partial melting of multicomponent systems of carbonate minerals are even lower than the geothermal ones. This may not limit a generation of carbonate parental media of deeper mantle diamonds. High capability for nucleation and mass crystallization of the multicomponent carbonate–carbon melts studied for the formation of deeper mantle diamonds is demonstrated in high-pressure high-temperature experiments.

**Acknowledgments** This work was funded by Program 12P/2 of Russian Academy of Sciences and Grants RFBR 13-05-00835, 14-05-31142.

## References

- Akaogi M (2007) Phase transitions of minerals in the transition zone and upper part of the lower mantle. In: Ohtani E (ed) *Advances in high-pressure mineralogy*. Geological society of America special paper 421. Geological society of America, Boulder, pp 1–13
- Boulard E, Glöter A, Corgne A, Antonangeli D, Auzende AL, Perrillat JP, Guyot F, Fiquet G (2011) New host for carbon in the deep Earth. *PNAS* 108(13):5184–5187. doi:10.1073/pnas.1016934108
- Brenker FE, Vollmer C, Vincze L, Vekemans B, Szymanski A, Janssens K, Szaloki I, Nasdala L, Kaminsky F (2007) Carbonates from the lower part of transition zone or even the lower mantle. *EPSL* 260:1–9. doi:10.1016/j.epsl.2007.02.038
- Bundy FP, Basset WA, Weathers MS, Hemley RJ, Mao H-K, Goncharov AF (1996) The pressure–temperature phase and transformation diagram for carbon updated through 1994. *Carbon* 34:141–153
- Dasgupta R, Hirschmann MM (2010) The deep carbon cycle and melting in Earth's interior. *EPSL* 298:1–13. doi:10.1016/j.epsl.2010.06.039
- Fiquet G, Guyot F, Kunz M, Matas J, Andrault D, Hanfland M (2002) Structural refinements of magnesite at very high pressure. *Am Miner* 87:1261–1265
- Frost DJ, Poe BT, Tronnes RG, Libsck C, Dube F, Rubie DC (2004) A new large-volume multianvil system. *PEPI* 143:507–514. doi:10.1016/j.pepi.2004.03.003
- Harte B (2010) Diamond formation in the deep mantle: the record of mineral inclusions and their distribution in relation to mantle dehydration zones. *Mineral Mag* 74(2):189–215. doi:10.1180/minmag.2010.074.2.189
- Isshiki M, Irifune T, Hirose K, Ono S, Ohishi Y, Watanuki T, Nishibori E, Takata M, Sakata M (2004) Stability of magnesite and its high-pressure form in the lowermost mantle. *Nature* 427:60–63. doi:10.1038/nature02181
- Kaminsky F (2012) Mineralogy of the lower mantle: a review of 'super-deep' mineral inclusions in diamond. *Earth Sci Rev* 110:127–147. doi:10.1016/j.earscirev.2011.10.005
- Litvin YuA (2009) The physicochemical conditions of diamond formation in the mantle matter: experimental studies. *Russian Geol Geophys* 50(12):1188–1200. doi:10.1016/j.rgg.2009.11.017
- Litvin YuA (2007) High-pressure mineralogy of diamond genesis. In: Ohtani E (ed) *Advances in high-pressure mineralogy*. Geological society of America special paper 241. Geological society of America, Boulder, pp 83–103
- Litvin YuA, Litvin VYu, Kadik AA (2008) Experimental characterization of diamond crystallization in melts of mantle silicate–carbonate–carbon systems at 7.0–8.5 GPa. *Geochem Intern* 46(6):531–553. doi:10.1134/S0016702908060013
- Litvin YuA, Vasiliev PG, Bobrov AV, Okoemova VYu, Kuzyura AV (2012) Parental media of natural diamonds and primary mineral inclusions in them: evidence from physicochemical experiment. *Geochem Int* 50(9):726–759. doi:10.1134/S0016702912070051
- Litvin YuA, Spivak AV, Solopova NA, Dubrovinsky LS (2014) On origin of lower-mantle diamonds and their primary inclusions. *PEPI* 228:176–185. doi:10.1016/j.pepi.2013.12.007
- McCammon C, Hutchison MT, Harris JW (1997) Ferric iron content of mineral inclusions in diamonds from São Luiz: a view into the lower mantle. *Science* 278:434–436. doi:10.1126/science.278.5337.434
- Merlini M, Crichton W, Hanfland M, Gemmi M, Mueller H, Kupenko I, Dubrovinsky L (2012) Structures of dolomite at ultrahigh pressure and their influence on the deep carbon cycle. *Proc Natl Acad Sci USA* 109(34):13509–13514. doi:10.1073/pnas.1201336109
- Santillan J, Williams Q (2004a) A high pressure X-ray diffraction study of aragonite and the post-aragonite phase transition in CaCO<sub>3</sub>. *Am Miner* 89:1348–1352
- Santillan J, Williams Q (2004b) A high-pressure infrared and X-ray study of FeCO<sub>3</sub> and MnCO<sub>3</sub>: comparison with CaMg(CO<sub>3</sub>)<sub>2</sub>-dolomite. *PEPI* 143:291–304. doi:10.1016/j.pepi.2003.06.007
- Skorodumova NV, Belonoshko AB, Huang L, Ahuja R, Johansson B (2005) Stability of the MgCO<sub>3</sub> structures under lower mantle conditions. *Am Miner* 90:1008–1011. doi:10.2138/am.2005.1685
- Solopova NA, Litvin YuA, Spivak AV, Dubrovinskaya NA, Dubrovinsky LS, Urusov VS (2013) Phase diagram of Na-carbonate, the alkaline component of growth media of the super-deep diamond. *Dokl Earth Sci* 453(1):1106–1109. doi:10.1134/S1028334X13110068
- Spivak AV, Dubrovinskii LS, Litvin YuA (2011) Congruent melting of calcium carbonate in a static experiment at 3500 K and 10–22 GPa: its role in the genesis of ultra-deep diamonds. *Dokl Earth Sci* 439(2):1171–1174. doi:10.1134/S1028334X11080319
- Spivak AV, Litvin YuA, Ovsyannikov SV, Dubrovinskaya N, Dubrovinsky LS (2012) Stability and breakdown of Ca<sup>13</sup>CO<sub>3</sub> melt associated with formation of <sup>13</sup>C-diamond in high-pressure static experiments up to 43 GPa and 3900 K. *J Solid State Chem* 19:102–106. doi:10.1016/j.jssc.2012.02.041
- Spivak AV, Solopova NA, Litvin YuA, Dubrovinsky LS (2013) Carbonate melts at lower mantle conditions: to superdeep diamonds genesis. *Mineral J (Ukraine)* 35(2):73–80 in Russian
- Stacey FD (1992) *Physics of the earth*, 3rd edn. Brookfield Press, Brisbane
- Stagno V, Tange Y, Miyajima N, McCammon CA, Irifune T, Frost DJ (2011) The stability of magnesite in the transition zone and the lower mantle as function of oxygen fugacity. *Geophys Res Lett* 38:L19309. doi:10.1029/2011GL049560